Japanese Journal of Radiology (2019) 37:412–419
https://doi.org/10.1007/s11604-019-00822-6

ORIGINAL ARTICLE

Liver assessment using Gd-EOB-DTPA-enhanced magnetic resonance imaging in primary biliary cholangitis patients

Dan Han[1] · Jiayi Liu[2] · Erhu Jin[1] · Wen He[1]

Received: 24 November 2018 / Accepted: 12 February 2019 / Published online: 23 February 2019

Abstract

Purpose To evaluate the feasibility of utilizing gadolinium ethoxybenzyl diethylenetriamine pentaacetic acid (Gd-EOB-DTPA)-enhanced magnetic resonance imaging (MRI) for the assessment of Child–Pugh class and for differentiating between patients with primary biliary cholangitis (PBC) and posthepatitic cirrhosis.

Materials and methods 45 PBC patients and 45 posthepatitic cirrhosis patients were enrolled and Gd-EOB-DTPA-enhanced MRI was applied. The average relative signal enhancement (RE) of the liver and average contrast to noise ratio (CNR) of common bile duct at 4, 20, and 50 min between different Child–Pugh classes of PBC patients were compared. The RE and CNR in all timepoints in patients with the same Child–Pugh class were compared between PBC patients and posthepatitic cirrhosis patients.

Results The RE of liver and CNR of common bile duct at 4, 20, and 50 min was significantly different between all Child–Pugh classes of PBC patients. There were also no significant differences in the RE of liver and CNR of common bile duct in all timepoints between patients with PBC and posthepatitic cirrhosis in the same Child–Pugh class.

Conclusion Gd-EOB-DTPA-enhanced MRI is feasible for liver function assessment in PBC patients. However, the ability of this modality in differentiating liver cirrhosis of different etiologies requires further investigation.

Keywords MRI · Gd-EOB-DTPA · Primary biliary cholangitis

Introduction

Primary biliary cholangitis (PBC) is an autoimmune disease of unknown etiology. PBC is characterized by high serum levels of anti-mitochondrial antibodies (AMA) and progressive non-suppurative inflammation of small- and medium-sized intrahepatic bile ducts, which could lead to cholestasis, peripylephlebitis, liver fibrosis, cirrhosis, and liver failure [1–4]. The natural history of PBC has gradually evolved over the past few decades, and has shown a tendency for delayed histological progression and improved overall survival rate with the use of ursodeoxycholic acid [4]. However, a considerable proportion of PBC patients show unsatisfactory treatment response to ursodeoxycholic acid. Due to the inevitable disease progression and subsequent complications, such patients require a more aggressive intervention [4]. Liver transplantation is the only effective treatment for end-stage PBC. Preoperative liver function assessment is essential to the success of the operation with a preference of noninvasive assessment. The most common clinical method way to assess liver function is Child–Pugh classification which includes hepatic encephalopathy, ascites, serum bilirubin, serum albumin, and prothrombin times. Nevertheless, it can only evaluate the overall liver function. On the other hand, preoperative structural imaging examinations are indispensable in revealing the other abnormalities out of liver in patients with liver disease. However, the feasibility of non-invasively assessing the liver function besides serum indexes remains to be elucidated. The later period of PBC is hepatocirrhosis with different pathological mechanisms from common cirrhosis. However, the possibility of differentiating PBC from common cirrhosis non-invasively remains largely unknown.

✉ Dan Han
hd7226021218@sina.com

[1] Department of Radiology, Beijing Friendship Hospital, Capital Medical University, Xicheng District, Beijing 100050, China

[2] Department of Radiology, Beijing Anzhen Hospital, Capital Medical University, Chaoyang District, Beijing 100029, China

Magnetic resonance imaging (MRI) is often applied for liver anatomical assessment [5–10], which provides high resolution with noninvasive and non-ionizing nature. Yet, conventional anatomical MRI only provides morphological details rather than functional information. With the recent introduction of liver-specific contrast agents, assessment of liver function by enhanced MRI is now possible. Gadolinium ethoxybenzyl diethylenetriamine pentaacetic acid (Gd-EOB-DTPA) is a liver-specific contrast agent, of which about 50% is taken up by hepatocytes and excreted into bile after intravenous administration. Thus, Gd-EOB-DTPA-enhanced MRI can be used to evaluate the structural and functional integrity of liver parenchyma and bile ducts. In addition, Gd-EOB-DTPA-enhanced MRI can reflect regional liver function, while conventional serum indexes can only evaluate the overall liver function [7, 11–13]. Previous studies have investigated the use of relative enhancement (RE) [14] and signal-to-noise ratio (SNR) [15] as parameters for assessment of liver function on Gd-EOB-DTPA-enhanced MRI, and some studies have proved Gadoxetic-acid contrast enhancement of cystic duct and common bile duct could be used as biomarkers to assess liver function [16]. Despite these MRI advancements, only one study has investigated the application of Gd-EOB-DTPA for assessment of liver function in patients with PBC [17]. More importantly, recent research on PBC has largely focused on the pathological staging and imaging characteristics [18], while none of these studies have assessed the use of contrast to noise ratio (CNR) as a measurement of liver function in patients with PBC. Furthermore, the feasibility of Gd-EOB-DTPA-enhanced MRI to differentiate patients with PBC and posthepatitic cirrhosis in the same Child–Pugh class remained unexplored. The aim of this study was to evaluate the liver function in patients PBC with different Child–Pugh classes using Gd-EOB-DTPA-enhanced MRI. In addition, we investigated the difference between PBC and posthepatitic cirrhosis using Gd-EOB-DTPA-enhanced MRI to explore the differences in pathological mechanisms.

Materials and methods

Patients

PBC patients and posthepatitic cirrhosis patients were divided into subgroups, according to Child–Pugh classifications [19, 20]. 45 PBC patients in Beijing Friendship Hospital from 2016 to Apr 2018 were prospectively enrolled in this study as experimental group (group A) and 45 posthepatitic cirrhosis patients (superinfection of hepatitis A and hepatitis B 16 cases, Viral hepatitis B 18 cases, Viral hepatitis C 9 cases, and Viral hepatitis D 2 cases) during this period were randomly selected as control group (group B). Among the PBC patients, 25, 11, and 9 were in Child Pugh A, Child Pugh B, and Child Pugh C, respectively. Among the posthepatitic cirrhosis patients, 21, 15, and 9 were in Child Pugh A, Child Pugh B, and Child Pugh C, respectively. The inclusion criteria for PBC patients were: (1) serum AMA titer $\geq$ 1:40; (2) unexplained increase in alkaline phosphatase $>$ 1.5 times the upper limit of normal for $>$ 24 weeks; and (3) compatible liver histological findings, such as non-suppurative cholangitis and interlobular bile duct injury [2, 21]. The exclusion criteria for PBC patients were: (1) patients with multiple focal lesions or patients with sum of longest diameter $>$ 5 cm (in cases of a few lesions); (2) thrombi or cancer emboli within portal vein and its major branches; (3) history of biliary tract surgery; and (4) patients with obstructive jaundice, severe hepatorenal dysfunction, severe ascites, and allergic predisposition [22–24]. For posthepatitic cirrhosis, the inclusion criteria were: (1) the course of acute hepatitis is more than half a year, or the original hepatitis B, C, D patients, or HBsAg carriers, and hepatitis symptoms, signs, and liver function abnormalities occur again due to the same pathogen or superinfection with another pathogen this time. (2) Diffuse hepatic fibrosis and nodule formation were the pathological manifestations of liver tissue [25]. The exclusion criteria for posthepatitic cirrhosis patients were: (1) autoimmune hepatitis; (2) comorbid conditions such as liver cancer or other severe liver or gallbladder diseases; and (3) severe comorbidity of heart, brain, kidney, or lung dysfunction [26, 27]. All liver function tests including serum albumin, total bilirubin and prothrombin time, assessment of ascites, and hepatic encephalopathy were conducted within 1 week of MRI evaluation for the purpose of Child–Pugh score assessment. The Committee of Medical Ethics of Beijing Friendship Hospital approved this study. Informed consent was obtained from all individual participants included in the study.

MR protocols

MRI data were collected using Signa Excite 3.0 T scanner (GE Healthcare, Little Chalfont, Buckinghamshire, UK) with an eight-channel torso array coil [28]. All subjects were made to fast for at least four hours immediately prior to the MRI examination. Gd-EOB-DTPA (Primovist®; Bayer Schering Pharma, Berlin, Germany, 0.025 mmol/kg) was injected intravenously at a rate of 1.0 mL/s and flushed by a bolus of saline (NaCl 0.9%) at the same rate. Array spatial sensitivity encoding technique (ASSET) sensitivity calibration was first performed, followed by breath-hold 3D fast spoiled gradient echo sequence (FSPGR) with liver acquisition with volume acceleration (LAVA) technique before contrast agent injection, and at 4, 20, and 50 min postinjection. The parameter of the FSPGR was repetition time (TR) = 2.8 ms, echo delay time (TE) = 1.2 ms, flip angle

= 12°, number of excitations = 0.8, slice thickness = 2 mm, spacing = − 1 mm, field of view (FOV) = 42 × 38 cm^2, and matrix size = 288 × 180 pixels.

Quantitative image analysis

Regions of interest (ROIs) with a size of 1 cm^2 were placed in the parenchyma of four liver segments at the level of the porta hepatis, which are left medial, left lateral, right anterior, and right posterior segments. Note that blood vessels, bile ducts, and small lesions were avoided. The relative enhancement (RE) between non-enhanced phase and 4, 20, and 50 min post-Gd-EOB-DTPA injection were calculated as per previously published standards [14]:

$$\mathrm{RE}\% = \left[(\text{SI-post} - \text{SI-pre})/\text{SI-pre}\right] \times 100\%, \quad (1)$$

where SI-pre and SI-post denote average signal intensity (SI) of four liver segments before and after contrast agent injection, respectively.

The SI in the center of common bile duct, the SI in the center of ipsilateral psoas major, and the standard deviation of the ipsilateral background noise were extracted from axial images. Contrast-to-noise ratio (CNR) of common bile duct 50 min after Gd-EOB-DTPA injection were calculated:

$$\mathrm{CNR} = (\mathrm{SI_{CBD}} - \text{SIpsoas major})/\mathrm{SD_{noise}}. \quad (2)$$

Qualitative image analysis

Two attending radiologists with more than 5 years of experience in diagnosing abdominal MRI graded the visualization of the MRI images with a 4-point scale: grade 4 for a well-enhancement liver parenchyma and bile duct lumen completely filled by intraluminal contrast with clearly outlined margins and excellent image quality, 3 for a moderately enhancement liver parenchyma and bile duct lumen with slightly obscured margin, good image quality, no artifacts, the influence of the noise and contrast agent concentration on images does not affect the evaluation of hepatic parenchyma and bile duct, 2 for a minimal liver parenchyma and bile duct lumen enhancement with ambiguous margin, artifacts, noise and contrast agent concentration have great influence on the images, but can meet the diagnostic requirements, and 1 for the poor image quality which cannot meet the diagnostic requirements. The doctors were blinded to the data on liver function classification and the type of liver cirrhosis.

Statistical analyses

Statistical analyses were carried out using SPSS version 22.0 (SPSS Inc., Chicago, USA). Continuous variables are presented as mean ± standard deviation (SD). Kappa test was employed to compare the visualization grade of the two radiologists in evaluating the MRI images. Multivariate Analysis of Variance (MANOVA) with least significant difference (LSD) test was employed for comparison of RE and CNR at different timepoints (4, 20, and 50 min after contrast agent injection) among all Child–Pugh classes in PBC patients, and RE and CNR between patients in the same Child–Pugh class in PBC patients and posthepatitic cirrhosis patients. $P < 0.05$ was considered to have significant difference.

Table 1 Clinical characteristics of study subjects and average liver signal intensity (mean ± SD) on non-enhanced MRI in patients with different Child–Pugh classes

Characteristics	PBC ($n = 45$)	Posthepatitic cirrhosis ($n = 45$)	P value
Age (years, mean ± SD)	53.7 ± 6.5	56.3 ± 7.0	0.072
Gender (*N*)			0.091
Male	20	28	
Female	25	17	
Child–Pugh class			0.618
A	25	21	
B	11	15	
C	9	9	
Average liver signal Intensity (mean ±SD) on non-enhanced MRI			
Child–Pugh A	368.51 ± 78.10	397.23 ± 72.84	0.403
Child–Pugh B	360.79 ± 71.10	403.89 ± 12.14	0.442
Child–Pugh C	407.67 ± 10.30	391.80 ± 10.56	0.401

SD standard deviation

Table 2 Visualization grade of the two radiologists (A and B) in evaluating the MRI images

Grade		B				Total
		1	2	3	4	
A	1	0	0	0	0	0
	2	1	0	1	0	2
	3	0	1	31	0	32
	4	0	0	1	55	56
Total		1	1	33	55	90

Kappa=0.909, $P < 0.001$

Results

There was no significant difference between the two groups with respect to age, sex, or SI on non-enhanced MRI (Table 1). The consistency of the two radiologists' visualization grade in evaluating the MRI images is very good (Kappa = 0.909, $P < 0.001$) (Table 2).

After Gd-EOB-DTPA injection, RE of liver and CNR of common bile duct at 4, 20, and 50 min was significantly different between all Child–Pugh classes in PBC patients

(Tables 3, 4). RE of liver and CNR of common bile duct at all timepoints tended to decrease with an increase in Child–Pugh class (Figs. 1, 2), with a significant difference of RE in liver ($P < 0.001$) and CNR in common bile duct ($P < 0.001$) in PBC patients with different Child–Pugh classes. Note that there was no significant difference in RE at 20 and 50 min within a particular Child–Pugh class in PBC patients ($P = 0.102$) (Table 3).

After Gd-EOB-DTPA injection, there was no significant difference in RE of liver ($P^{group} = 0.068$, Table 5) and CNR of common bile duct ($P^{group} = 0.905$, Table 6) at all timepoints after Gd-EOB-DTPA injection between patients with PBC and posthepatitic cirrhosis.

Table 3 RE of liver (mean ± SD) at 4, 20, and 50 min after Gd-EOB-DTPA injection in PBC patients

Time	Child–Pugh A	Child–Pugh B	Child–Pugh C	P	$P^{A\ vs\ B}$	$P^{A\ vs\ C}$	$P^{B\ vs\ C}$
4 min (a)	0.632 ± 0.048	0.362 ± 0.036	0.199 ± 0.610	< 0.001	< 0.001	< 0.001	< 0.001
20 min (b)	0.840 ± 0.065	0.475 ± 0.018	0.329 ± 0.046	< 0.001	< 0.001	< 0.001	< 0.001
50 min (c)	0.861 ± 0.065	0.492 ± 0.023	0.344 ± 0.041	< 0.001	< 0.001	< 0.001	< 0.001
P	< 0.001	< 0.001	< 0.001				
$P^{a\ vs\ b}$	< 0.001	< 0.001	< 0.001				
$P^{a\ vs\ c}$	< 0.001	< 0.001	< 0.001				
$P^{b\ vs\ c}$	0.216	0.145	0.529				

Total $P^{Child-Pugh} < 0.001$, $P^{time} < 0.001$, $P^{a\ vs\ b} < 0.001$, $P^{a\ vs\ c} < 0.001$, $P^{b\ vs\ c} = 0.102$, $P^{A\ vs\ B} < 0.001$, $P^{A\ vs\ C} < 0.001$, $P^{B\ vs\ C} < 0.001$

Table 4 CNR of common bile duct (mean ± SD) at 4, 20, and 50 min after Gd-EOB-DTPA injection in PBC patients

Time	Child–Pugh A	Child–Pugh B	Child–Pugh C	P	$P^{A\ vs\ B}$	$P^{A\ vs\ C}$	$P^{B\ vs\ C}$
4 min(a)	10.722 ± 0.420	8.624 ± 0.204	2.497 ± 0.283	< 0.001	< 0.001	< 0.001	< 0.001
20 min(b)	15.830 ± 0.445	10.543 ± 0.266	3.635 ± 0.210	< 0.001	< 0.001	< 0.001	< 0.001
50 min(c)	18.312 ± 0.626	12.594 ± 0.592	5.145 ± 0.289	< 0.001	< 0.001	< 0.001	< 0.001
P	< 0.001	< 0.001	< 0.001				
$P^{a\ vs\ b}$	< 0.001	< 0.001	< 0.001				
$P^{a\ vs\ c}$	< 0.001	< 0.001	< 0.001				
$P^{b\ vs\ c}$	< 0.001	< 0.001	< 0.001				

Total $P^{Child-Pugh} < 0.001$, $P^{time} < 0.001$, $P^{a\ vs\ b} < 0.001$, $P^{a\ vs\ c} < 0.001$, $P^{b\ vs\ c} < 0.001$, $P^{A\ vs\ B} < 0.001$, $P^{A\ vs\ C} < 0.001$, $P^{B\ vs\ C} < 0.001$

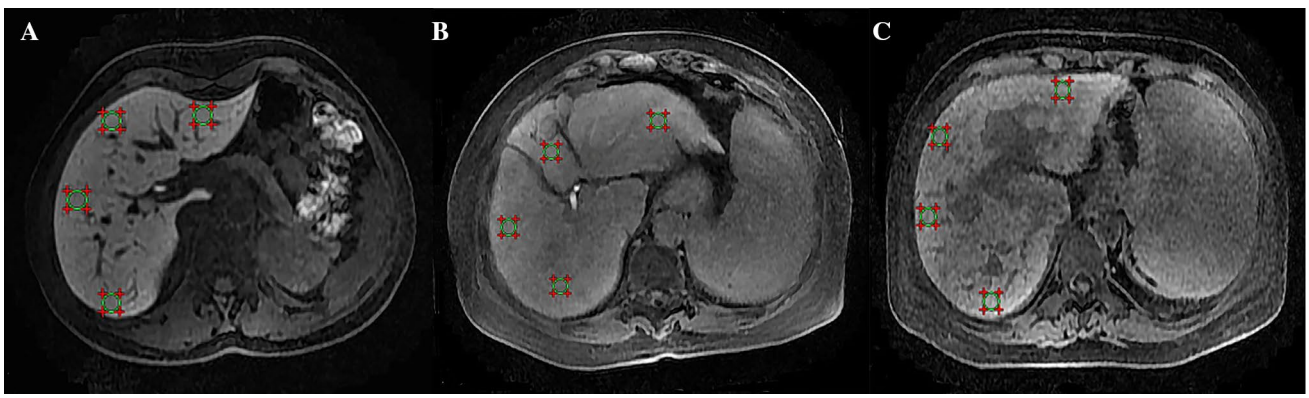

Fig. 1 Enhance performance of liver at 20 min after contrast agent injection was significantly different in PBC patients with different Child–Pugh classes and average SI of liver decrease with increase in Child–Pugh class **a** Child–Pugh class A, 45-year-old female; **b** Child–Pugh class B, 52-year-old male; **c** Child–Pugh class C, 56-year-old male. Regions of interest are indicated by circles to measure the SI of liver

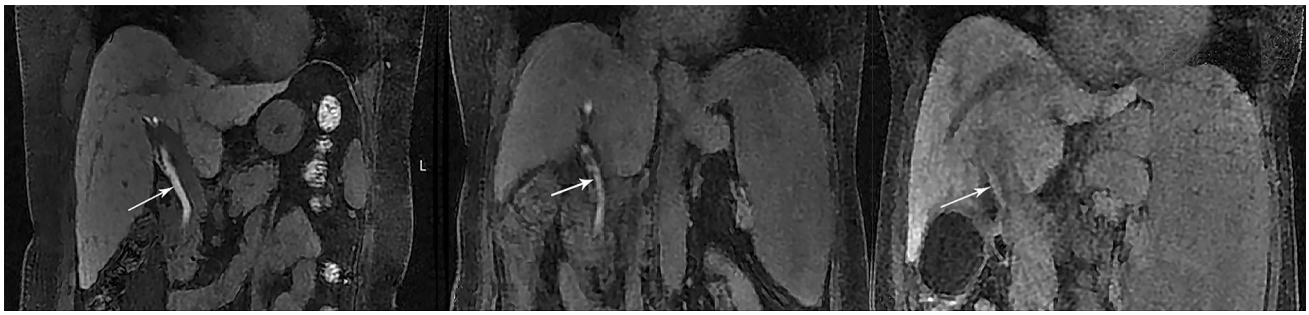

Fig. 2 50 min after contrast agent injection, the enhance performance of common bile duct decreased with increase of Child–Pugh class in PBC patient. **a** Child–Pugh class A, 45-year-old female; **b** Child–Pugh class B, 52-year-old male; **c** Child–Pugh class C, 56-year-old male. Regions of interest are common bile duct. The coronal images can show the enhance performance of common bile duct in longer range

Table 5 RE (mean ± SD) between patients at 4, 20, and 50 min after Gd-EOB-DTPA injection in group A and B

Time	Group A			Group B		
	Child–Pugh A	Child–Pugh B	Child–Pugh C	Child–Pugh A	Child–Pugh B	Child–Pugh C
4 min (a)	0.632 ± 0.048	0.362 ± 0.036	0.199 ± 0.610	0.663 ± 0.040	0.356 ± 0.027	0.233 ± 0.002
20 min (b)	0.840 ± 0.065	0.475 ± 0.018	0.329 ± 0.046	0.865 ± 0.049	0.472 ± 0.010	0.319 ± 0.008
50 min (c)	0.861 ± 0.065	0.492 ± 0.023	0.344 ± 0.041	0.878 ± 0.050	0.480 ± 0.023	0.326 ± 0.011

$P^{group} = 0.068$

Table 6 CNR (mean ±SD) between patients at 4, 20, and 50 min after Gd-EOB-DTPA injection in groups A and B

Time	Group A			Group B		
	Child–Pugh A	Child–Pugh B	Child–Pugh C	Child–Pugh A	Child–Pugh B	Child–Pugh C
4 min (a)	10.722 ± 0.420	8.624 ± 0.204	2.497 ± 0.283	10.666 ± 0.135	8.598 ± 0.327	2.501 ± 0.218
20 min (b)	15.830 ± 0.445	10.543 ± 0.266	3.635 ± 0.210	15.712 ± 0.262	10.615 ± 0.354	3.433 ± 0.301
50 min (c)	18.312 ± 0.626	12.594 ± 0.592	5.145 ± 0.289	18.489 ± 0.573	12.818 ± 0.663	5.183 ± 0.605

P^{group}=0.905

Discussion

Recent advances in laboratory techniques have improved the diagnosis and treatment of PBC [29]. However, imaging modalities for liver function assessment in these patients remain largely unexplored. The introduction of hepatobiliary-system-specific magnetic resonance contrast agents Gd-EOB-DTPA has allowed the use of enhanced MRI for evaluation of hepatic function in clinical settings. However, the application of enhanced MRI for liver functional assessment in patients with PBC is not well-characterized in the previous study [17]. In this study, we sought to investigate the feasibility of assessing PBC patients with different liver functions, and explored the potential difference between PBC patients and posthepatitic cirrhosis patients using Gd-EOB-DTPA contrast enhanced MRI.

Among patients with PBC, we observed a decrease in both RE and CNR with increase in Child–Pugh class. RE of liver and CNR of common bile duct did not show significant differences in patients with liver cirrhosis of different etiologies who are in the same Child–Pugh class. The above findings indicate that Gd-EOB-DTPA-enhanced MRI can be used to assess liver functions, yet the performance of Gd-EOB-DTPA-enhanced MRI may not be able to distinguish liver cirrhosis of different etiologies.

Gd-EOB-DTPA is a paramagnetic contrast agent, which reduces spin–lattice relaxation time. It is derived from Gd-DTPA, and has an additional lipophilic group (EOB) linked to the DTPA backbone. This allows it to be readily taken up by hepatocytes [30–32]. Following an intravenous injection, around half of Gd-EOB-DTPA is transferred into functional hepatocytes by organic anion-transporting

polypeptide OATP1B1/OATP1B3 and subsequently excreted in to the bile by multidrug resistance-associated protein 2. The remaining half of Gd-EOB-DTPA is excreted through the renal system [33]. In the previous studies, the uptake process starts 1.5 min after contrast agent injection, while peak liver parenchymal enhancement is observed at about 20 min [34]. Note that peak common bile duct enhancement is observed at 40–50 min postcontrast agent injection [35]. For optimal evaluation of the liver function, two timepoints (20 and 50 min) were chosen for the main hepatobiliary phases of this study.

Recent studies have evaluated multiple parameters for liver function assessment, but most of these studies mainly focused on changes in SI postcontrast agent injection [14, 36–40]. However, SI may not be an entirely objective measurement as, it can be affected by various factors, including the inhomogeneity of the magnetic field (B_0), radiofrequency pulse (B_1), repetition time (TR), and echo time (TE). We investigated RE according to the methodology used in previously published studies [14, 15], in which the protocols were RE and CNR of common bile duct at 4, 20, and 50 min after contrast agent injection. Relative enhancement is a ratio of SI enhancement, while CNR represents the ratio of the difference of SI between common bile duct and psoas major and SD of adjacent background noise. Therefore, both these parameters tend to improve reliability by minimizing the influences of different models and inaccurate SI. Since MRI signals may vary in different hepatic segments due to chronic pathological changes in PBC, we employed an average SI of four liver segments at the level of porta hepatis in this study, so that the data are more representative of the overall liver function.

Our results indicate that RE and CNR changes were consistent with Child–Pugh class in patients with PBC. RE and CNR of common bile duct at all timepoints tended to decrease with increase in Child–Pugh class. This finding is consistent with the previous study [17, 39], indicating that Gd-EOB-DTPA-enhanced MRI can be feasible for liver function assessment. Child–Pugh score essentially reflects the degree of liver dysfunction [41], which could be a result of OATP1B3 downregulation [42]. Down-regulated OATP1B3 also impairs Gd-EOB-DTPA uptake and excretion, thereby decreasing Gd-EOB-DTPA concentration. This is reflected in the typical findings of reduced RE and CNR in patients with PBC. Nonetheless, RE at 20 and 50 min after contrast agent injection were not significantly different in PBC patients within every Child–Pugh class. This indicates that hepatocytes could be saturated with Gd-EOB-DTPA, and therefore, a delay of 20 min is adequate for liver function assessment. This finding is consistent with the prior study [39]. In this study, there was significant difference in CNR of common bile duct at 4, 20 and 5,0 min within a particular Child–Pugh class in PBC patients, and the CNR tended to increase with an increase time and peak common bile duct enhancement is observed at 50 min. This finding is also consistent with the prior study [35]. Furthermore, we observed that RE and CNR of common bile duct at all timepoints after contrast agent injection were similar between patients with PBC and posthepatitic cirrhosis in the same Child–Pugh class. This illustrates that RE of liver and CNR of common bile duct are mainly related to liver function rather than to cholestasis and excretion dysfunction of intrahepatic small bile ducts.

It is pertinent to mention some limitations of Gd-EOB-DTPA-enhanced MRI and this study. Gd-EOB-DTPA-enhanced MRI can be affected by individual genetic polymorphism. A previous study showed that single nucleotide polymorphisms of OATPB1 and OATPB3 could impair the liver uptake ability and lower the degree of liver enhancement. Therefore, genetic polymorphism may also potentially account for the variability of SI in the hepatobiliary phases. This factor potentially compromises the accuracy of liver function assessment and may also explain the inter-individual differences. To minimize this effect, we employed average of SI in four liver segments. In this study, the small sample size of patients with PBC and in subgroups based on the Child–Pugh class is another disadvantage which limits the statistical power of the analysis. Further studies with a larger sample of patients in each particular Child–Pugh class are required to solidify our findings.

In conclusion, Gd-EOB-DTPA-enhanced MRI, a non-invasive modality, is feasible for liver function assessment in patients with PBC. This can be a valuable supplement to clinical evaluation besides using Child–Pugh class with an advantage of regional liver function evaluation. However, the ability and accuracy of this modality in differentiating liver cirrhosis of different etiologies require further investigation.

Acknowledgements We thank Yi Zhang, Ligang Deng, Wei Guan, and Guilian Jiang for their technical assistance in performing the MRI images. The authors also appreciate the help of the teachers who work in the Medical records room, because they provide us with great convenience in looking up patients' clinical data.

Funding This study was approved by the Health Industry Special Scientific Research Project (No. 201402019).

Compliance with ethical standards

Conflict of interest The authors declare that they have no conflict of interest.

Ethical approval This study was approved by the Ethics Committee of Beijing Friendship Hospital, Capital Medical University.

Ethical statement All procedures performed in studies involving human participants were in accordance with the ethical standards of the institutional and/or national research committee and with the 1964

Helsinki declaration and its later amendments or comparable ethical standards.

Informed consent Informed consent was obtained from all individual participants included in the study.

References

1. Crosignani A, Battezzati PM, Invernizzi P, Selmi C, Prina E, Podda M. Clinical features and management of primary biliary cirrhosis. World J Gastroenterol: WJG. 2008;14(21):3313–27.
2. Lindor KD, Gershwin ME, Poupon R, Kaplan M, Bergasa NV, Heathcote EJ. Primary biliary cirrhosis. Hepatology. 2009;50(1):291–308.
3. Nguyen DL, Juran BD, Lazaridis KN. Primary biliary cirrhosis. Best Pract Res Clin Gastroenterol. 2010;24(5):647–54.
4. Selmi C, Bowlus CL, Gershwin ME, Coppel RL. Primary biliary cirrhosis. Lancet. 2011;377(9777):1600–9.
5. Stockmann M, Lock JF, Riecke B, Heyne K, Martus P, Fricke M, et al. Prediction of postoperative outcome after hepatectomy with a new bedside test for maximal liver function capacity. Ann Surg. 2009;250(1):119–25.
6. de Graaf W, van Lienden KP, Dinant S, Roelofs JJ, Busch OR, Gouma DJ, et al. Assessment of future remnant liver function using hepatobiliary scintigraphy in patients undergoing major liver resection. J Gastrointest Surg. 2010;14(2):369–78.
7. An SK, Lee JM, Suh KS, Lee NJ, Kim SH, Kim YJ, et al. Gadobenate dimeglumine-enhanced liver MRI as the sole preoperative imaging technique: a prospective study of living liver donors. AJR Am J Roentgenol. 2006;187(5):1223–33.
8. Sanuki N, Takeda A, Oku Y, Eriguchi T, Nishimura S, Aoki Y, et al. Threshold doses for focal liver reaction after stereotactic ablative body radiation therapy for small hepatocellular carcinoma depend on liver function: evaluation on magnetic resonance imaging with Gd-EOB-DTPA. Int J Radiat Oncol Biol Phys. 2014;88(2):306–11.
9. Nilsson H, Karlgren S, Blomqvist L, Jonas E. The inhomogeneous distribution of liver function: possible impact on the prediction of post-operative remnant liver function. HPB. 2015;17(3):272–7.
10. Xie S, Sun Y, Wang L, Yang Z, Luo J, Wang W. Assessment of liver function and liver fibrosis with dynamic Gd-EOB-DTPA-enhanced MRI. Acad Radiol. 2015;22(4):460–6.
11. Tajima T, Akahane M, Takao H, Akai H, Kiryu S, Imamura H, et al. Detection of liver metastasis: is diffusion-weighted imaging needed in Gd-EOB-DTPA-enhanced MR imaging for evaluation of colorectal liver metastases? Jpn J Radiol. 2012;30(8):648–58.
12. Tateyama A, Fukukura Y, Takumi K, Shindo T, Kumagae Y, Kamimura K, et al. Gd-EOB-DTPA-enhanced magnetic resonance imaging features of hepatic hemangioma compared with enhanced computed tomography. World J Gastroenterol. 2012;18(43):6269–76.
13. Bashir MR, Gupta RT, Davenport MS, Allen BC, Jaffe TA, Ho LM, et al. Hepatocellular carcinoma in a North American population: does hepatobiliary MR imaging with Gd-EOB-DTPA improve sensitivity and confidence for diagnosis? J Magn Reson Imaging. 2013;37(2):398–406.
14. Shimizu J, Dono K, Gotoh M, Hasuike Y, Kim T, Murakami T, et al. Evaluation of regional liver function by gadolinium-EOB-DTPA-enhanced MR imaging. Dig Dis Sci. 1999;44(7):1330–7.
15. Papanikolaou N, Prassopoulos P, Eracleous E, Maris T, Gogas C, Gourtsoyiannis N. Contrast-enhanced magnetic resonance cholangiography versus heavily T2-weighted magnetic resonance cholangiography. Invest Radiol. 2001;36(11):682–6.
16. Noda Y, Goshima S, Kajita K, Kawada H, Kawai N, Koyasu H, et al. Biliary tract enhancement in gadoxetic acid-enhanced MRI correlates with liver function biomarkers. Eur J Radiol. 2016;85(11):2001–7.
17. Nilsson H, Blomqvist L, Douglas L, Nordell A, Jonas E. Assessment of liver function in primary biliary cirrhosis using Gd-EOB-DTPA-enhanced liver MRI. HPB. 2010;12(8):567–76.
18. Kobayashi S, Matsui O, Gabata T, Terayama N, Sanada J, Yamashiro M, et al. MRI findings of primary biliary cirrhosis: correlation with Scheuer histologic staging. Abdom Imaging. 2005;30(1):71–6.
19. Forman LM, Lucey MR. Predicting the prognosis of chronic liver disease: an evolution from child to MELD Mayo End-stage Liver Disease. Hepatology. 2001;33(2):473–5.
20. Zhou HY, Chen TW, Zhang XM, Jing ZL, Zeng NL, Zhai ZH. Patterns of portosystemic collaterals and diameters of portal venous system in cirrhotic patients with hepatitis B on magnetic resonance imaging: Association with Child-Pugh classifications. Clin Res Hepatol Gastroenterol. 2015;39(3):351–8.
21. Heathcote EJ. Management of primary biliary cirrhosis. The American Association for the Study of Liver Diseases practice guidelines. Hepatology. 2000;31(4):1005–133.
22. Purohit T, Cappell MS. Primary biliary cirrhosis: Pathophysiology, clinical presentation and therapy. World J Hepatol. 2015;7(7):926–41.
23. Marchioni Beery RM, Vaziri H, Forouhar F. Primary biliary cirrhosis and primary sclerosing cholangitis: a review featuring a women's health perspective. J Clin Transl Hepatol. 2014;2(4):266–84.
24. Gulamhusein AF, Juran BD, Lazaridis KN. Genome-wide association studies in primary biliary cirrhosis. Semin Liver Dis. 2015;35(4):392–401.
25. Chinese Society of Hepatology and Chinese Society of Infectious Diseases CMA. The guideline of prevention and treatment for chronic hepatitis. Chin Hepatol. 2005;10:348-57.
26. Wang L, Su Y, Zhang Q, Liu P, Su SB. Classification and modeling of traditional Chinese medicine syndromes in patients with post-hepatitic cirrhosis by partial least-squares. Zhong Xi Yi Jie He Xue Bao. 2008;6(11):1122–8.
27. Zhang H, Lv H, Huang PX, Lin Y, Hu XC, Liu P. Comparative study of TCM syndrome scale for liver disease and chronic liver disease questionnaire based on assessment of posthepatitic cirrhosis. Evid Based Complement Alternat Med. 2012;2012:496575.
28. Kobayashi S, Matsui O, Gabata T, Koda W, Minami T, Kozaka K, et al. Intrahepatic periportal high intensity on hepatobiliary phase images of Gd-EOB-DTPA-enhanced MRI: imaging findings and prevalence in various hepatobiliary diseases. Jpn J Radiol. 2013;31(1):9–15.
29. Shi J, Wu C, Lin Y, Chen YX, Zhu L, Xie WF. Long-term effects of mid-dose ursodeoxycholic acid in primary biliary cirrhosis: a meta-analysis of randomized controlled trials. Am J Gastroenterol. 2006;101(7):1529–38.
30. Do RK, Rusinek H, Taouli B. Dynamic contrast-enhanced MR imaging of the liver: current status and future directions. Magn Reson Imaging Clin N Am. 2009;17(2):339–49.
31. Gschwend S, Ebert W, Schultze-Mosgau M, Breuer J. Pharmacokinetics and imaging properties of Gd-EOB-DTPA in patients with hepatic and renal impairment. Invest Radiol. 2011;46(9):556–66.
32. Lee NK, Kim S, Kim GH, Heo J, Seo HI, Kim TU, et al. Significance of the "delayed hyperintense portal vein sign" in the hepatobiliary phase MRI obtained with Gd-EOB-DTPA. J Magn Reson Imaging. 2012;36(3):678–85.

33. Goodwin MD, Dobson JE, Sirlin CB, Lim BG, Stella DL. Diagnostic challenges and pitfalls in MR imaging with hepatocyte-specific contrast agents. Radiographics. 2011;31(6):1547–68.
34. Vogl TJ, Kummel S, Hammerstingl R, Schellenbeck M, Schumacher G, Balzer T, et al. Liver tumors: comparison of MR imaging with Gd-EOB-DTPA and Gd-DTPA. Radiology. 1996;200(1):59–67.
35. Dahlstrom N, Persson A, Albiin N, Smedby O, Brismar TB. Contrast-enhanced magnetic resonance cholangiography with Gd-BOPTA and Gd-EOB-DTPA in healthy subjects. Acta Radiol. 2007;48(4):362–8.
36. Kanki A, Tamada T, Higaki A, Noda Y, Tanimoto D, Sato T, et al. Hepatic parenchymal enhancement at Gd-EOB-DTPA-enhanced MR imaging: correlation with morphological grading of severity in cirrhosis and chronic hepatitis. Magn Reson Imaging. 2012;30(3):356–60.
37. Katsube T, Okada M, Kumano S, Hori M, Imaoka I, Ishii K, et al. Estimation of liver function using T1 mapping on Gd-EOB-DTPA-enhanced magnetic resonance imaging. Invest Radiol. 2011;46(4):277–83.
38. Motosugi U, Ichikawa T, Sou H, Sano K, Tominaga L, Kitamura T, et al. Liver parenchymal enhancement of hepatocyte-phase images in Gd-EOB-DTPA-enhanced MR imaging: which biological markers of the liver function affect the enhancement? J Magn Reson Imaging. 2009;30(5):1042–6.
39. Nakamura S, Awai K, Utsunomiya D, Namimoto T, Nakaura T, Morita K, et al. Chronological evaluation of liver enhancement in patients with chronic liver disease at Gd-EOB-DTPA-enhanced 3-T MR imaging: does liver function correlate with enhancement? Jpn J Radiol. 2012;30(1):25–33.
40. Tajima T, Takao H, Akai H, Kiryu S, Imamura H, Watanabe Y, et al. Relationship between liver function and liver signal intensity in hepatobiliary phase of gadolinium ethoxybenzyl diethylenetriamine pentaacetic acid-enhanced magnetic resonance imaging. J Comput Assist Tomogr. 2010;34(3):362–6.
41. Huo TI, Lin HC, Wu JC, Lee FY, Hou MC, Lee PC, et al. Proposal of a modified Child-Turcotte-Pugh scoring system and comparison with the model for end-stage liver disease for outcome prediction in patients with cirrhosis. Liver Transpl. 2006;12(1):65–71.
42. Narita M, Hatano E, Arizono S, Miyagawa-Hayashino A, Isoda H, Kitamura K, et al. Expression of OATP1B3 determines uptake of Gd-EOB-DTPA in hepatocellular carcinoma. J Gastroenterol. 2009;44(7):793–8.